Advances in Geo-Energy Research

Vol. 14, No. 2, p. 135-146, 2024

Original article

In-situ emulsification and viscosification system of surfactant-assisted Janus nanofluid and its profile control effect

Hairong Wu[1], Jiawei Chang[1], Guorui Xu[2], Wenhao Shao[1], Genglin Li[3], Jirui Hou[1]*

[1]*State Key Laboratory of Petroleum Resources and Engineering, China University of Petroleum (Beijing), Beijing 102249, P. R. China*

[2]*COSL Production Optimization, China Oilfield Services Limited, Tianjin 300452, P. R. China*

[3]*Department of Chemical and Materials Engineering, University of Alberta, Edmonton, Alberta T6G 1H9, Canada*

Keywords:
Janus nanoparticle
emulsification
viscosification
water in oil emulsion
profile control
dispersion stability

Cited as:
Wu, H., Chang, J., Xu, G., Shao, W., Li, G., Hou, J. *In-situ* emulsification and viscosification system of surfactant-assisted Janus nanofluid and its profile control effect. Advances in Geo-Energy Research, 2024, 14(2): 135-146.
https://doi.org/10.46690/ager.2024.11.06

Abstract:
To construct the *in-situ* emulsification and viscosification system that is suitable for low permeability oil reservoirs characterized by high-temperature and high-salt, the amphiphilic Janus SiO_2 nanoparticles and Tween 60/Imidazoline oleate surfactant system were combined. The mechanism of *in-situ* emulsification and viscosification system was elucidated from two aspects: The dynamic adsorption and phase conversion of surfactant, and the unique bridge structure of Janus nanoparticle stabilized emulsion. The successful synthesis of Janus SiO_2 nanoparticles with varying degrees of hydrophilicity and hydrophobicity was achieved through regulating the reaction conditions. Based on emulsion stability, the optimization of the modification degree of Janus SiO_2 nanoparticles was achieved. The *in-situ* emulsification and viscosification system was constructed by introducing Tween 60/Imidazoline oleate as dispersion aid agent and emulsifier. Notably, the *in-situ* emulsification and viscosification system can be stably dispersed for more than 12 hours in high-temperature and high-salt. The dispersion stability of the *in-situ* emulsification and viscosification system was evaluated qualitatively by visual inspection, Turbiscan stability index and monitoring particle size. The emulsification ability, emulsion stability and rheological properties of the systems with different concentrations were evaluated at 90 °C and a salinity of 35,000 ppm. It was found that the *in-situ* emulsification and viscosification system with the concentration of 0.64 wt% shows better profile control and enhanced recovery performance. This study presents a new approach for profile control using amphiphilic Janus nanoparticles and provides a promising prospect for applying nanoparticles in the field of enhanced oil recovery.

1. Introduction

To improve the recovery of crude oil, the application of long-term water flooding has resulted in a series of problems such as water cones, water channeling and fingering. This phenomenon entails the injection water forcefully infiltrating the oil well through channels with high permeability, thereby resulting in a decreased efficiency of water flooding (Li et al., 2020a). Profile control technology is a water control and oil stabilization technique that has the capability to effectively impede the movement of fluids through high permeability layers. Water-in-oil (W/O) emulsions with varying viscosities can be generated under distinct water containing conditions through the utilization of *in-situ* emulsification and viscosification technology (Pang et al., 2018; Chen et al., 2024). The preparation of a high viscosity W/O emulsion within the high water cut seepage channel serves to effectively obstruct the primary channel, control the oil-water distribution, and enlarge the overall volume of the reservoir's macroscopic waves. Due

Yandy Scientific Press

*Corresponding author.
E-mail address: wuhairong-123@163.com (H. Wu); cjw19980714@163.com (J. Chang); xugr@cosl.com.cn (G. Xu); swhx0904@163.com (W. Shao); genglin@ualberta.ca (G. Li); houjirui@126.com (J. Hou).

Received September 7, 2024; revised October 2, 2024; accepted October 24, 2024; available online October 28, 2024.

Table 1. Composition of simulated formation water.

Ion	Cl^-	HCO_3^-	SO_4^{2-}	Ca^{2+}	Mg^{2+}	Na^++K^+	Total salinity
Concentration (mg/L)	19,457	226	1,619	439	1,211	10,686	35,000

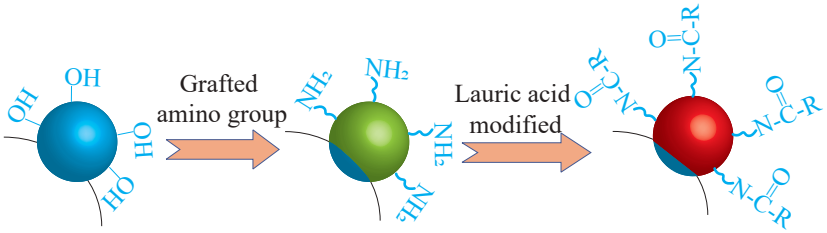

Fig. 1. The synthesis process of Janus amphiphilic nanoparticles by Pickering emulsion method.

to its surface activity and capacity to diminish the interfacial tension (IFT) between water and oil, the system exhibits the potential to enhance the microscopic oil flooding efficiency (Cao et al., 2022; Shen et al., 2023).

The stability of the emulsion is the guarantee for the successful application of this technique. Typically, surfactants, surface homogenization modified nanoparticles are employed as emulsifiers and stabilizers for traditional *in-situ* emulsification and viscosification system (Chen et al., 2014; Guo et al., 2022). However, with the development of the reservoirs with more extreme conditions, higher requirements are put forward for the temperature- and salt-resistant properties of oil displacing agents (Li et al., 2021a; Yang et al., 2023a, 2023b). The emulsion generated by a typical surfactant system exhibits inadequate emulsification capacity and emulsion stability when subjected to elevated temperatures and high salinity conditions (Lu et al., 2023a). The irreversible adsorption of nanoparticles at the water-oil interface, attributed to their high adsorption energy, contributes to the favorable emulsion stability observed in Pickering emulsions (Choi et al., 2023). Nevertheless, research findings indicate that the emulsification efficacy of individual homogeneous modified nanoparticles is substandard, resulting in emulsions that demonstrate inadequate stability when subjected to the simultaneous influence of elevated temperature and salinity levels (Krishnakumar and Elansezhian, 2022; Yarveicy, 2023).

Amphiphilic Janus nanoparticles are characterized by hydrophilic and oleophilic properties on both sides of the nanoparticles (Jia et al., 2021). The unique architecture of Janus nanoparticles enables their spontaneous adsorption, leading to the development of a dense adsorption layer at the oil-water interface. Hence, amphiphilic Janus nanoparticles exhibit enhanced emulsifying characteristics and improved stability of emulsions. The experimental findings indicate that emulsions stabilized by Janus nanoparticles exhibit characteristics of both kinetic and thermodynamic stability. In contrast, Pickering emulsions stabilized by homogeneous modified nanoparticles primarily demonstrate kinetic stability (Kumar et al., 2013). The enhanced interfacial activity exhibited by Janus nanoparticles, along with their superior stability in W/O emulsions, renders them suitable for utilization in *in-situ* emulsification and viscosification systems.

In this study, an *in-situ* emulsification and viscosification system was established by combining the Janus SiO_2 nanoparticles with nonionic/zwitterionic surfactants surfactant. Based on dispersion stability, the *in-situ* emulsification and viscosification system is constructed to ensure its stable performance at high-salinity and high-temperature conditions. In particular, the controllable adjustment mechanism of Janus nanoparticles and *in-situ* emulsification mechanism are described in detail, which provides a theoretical basis for the subsequent design of *in-situ* emulsification and viscosification systems. This study introduces a novel approach for utilizing amphiphilic Janus nanoparticles in reservoir profile control.

2. Materials and methods

2.1 Materials

Janus SiO_2 nanoparticles (15 nm, Laboratory preparation) was prepared according to previous work (Wu et al., 2020). Polyoxymethylene sorbitol anhydride monostearate (Tween 60, AR) and Imidazoline oleate (IO, with purity of 97%) were both purchased from Shanghai Maclean Biochemical Technology Co., LTD. The viscosity of crude oil applied is 33 mPa·s at 90 °C. The composition parameters of simulated formation water are shown in Table 1. The diameter of the cores used in the core-flooding experiment was $4.5 \times 4.5 \times 30$ cm^3. The water permeability of three cores used in the experiment were 38, 72 and 189 mD.

2.2 Characterization and optimization of the modification degree

The Janus SiO_2 nanoparticles were synthesized using the Pickering emulsion method. The preparation process consists of two distinct stages: amino acid modification and lauric acid modification. Additionally, two steps were undertaken to regulate the degree of surface modification, as depicted in Fig. 1. The degree of surface modification of Janus SiO_2 nanoparticles was regulated during the synthesis process through the manipulation of various parameters, including reaction time, concentration of reactants, pH value, and reaction temperature. The changes in the specific reaction parameters are illustrated

Table 2. Experimental conditions for control of the degree of amino modification.

	Time (h)	Temperature (°C)	KH550 (g)
Amino group modification	2, 4, 6, 8	30, 40, 50	2, 4, 6, 8

Table 3. Control experimental conditions for the degree of lauric acid modification.

	Time (h)	Lauric acid (g)	pH	EDC (g)
Modification by lauric acid	9, 12, 15, 18	30, 40, 50	6, 8	2, 4, 6, 8

in Tables 2 and 3.

The acid-base titration method and sessile drop method measuring contact angle were adopted for amino and lauric acid modified characterization.

Acid-base titration was performed according to method reported by Li et al. (2021b). The amount of 0.2 g amino modified Janus SiO_2 nanoparticles was dissolved in the mixture of absolute ethanol and 20% NaCl aqueous solution for subsequent experiments. The Janus SiO_2 nanoparticles were uniformly dispersed in the water using ultrasound until the nanoparticles were evenly dispersed. The pH value of the mixed solution was adjusted to 4 by 0.01 mol/L HCl solution. Once the pH value reached 4, no substantial alterations were observed within one minute. Subsequently, the concentration of a 0.01 mol/L NaOH solution was incrementally introduced through dropwise addition. The Janus SiO_2 nanoparticle mixture system was titrated by 0.01 mol/L NaOH solution until the pH of the system reached a value of 9 and remained constant for a duration of 1 minutes. The quantity of NaOH consumed was determined by the quantity of silica hydroxyl groups present of SiO_2 nanoparticles. Accordingly, the degree of modification could be reflected by the amount of NaOH consumed.

Sessile drop method was employed for measuring contact angle. Powder of nanoparticles with various lauric acid chain grafting degrees was fabricated into thin slices using the powder pelleting machine. Surface contact angles of Janus SiO_2 nanoparticles thin slices were characterized at 25 °C using Teclis interface rheometer (Traker-S, France). The liquid phase used in the experiment is deionized water.

The selection of suitable amphiphilic Janus SiO_2 nanoparticles for the *in-situ* emulsification and viscosification system was determined by evaluating the stability of W/O emulsions stabilized using various hydrophilic and hydrophobic Janus SiO_2 nanoparticles.

2.3 Performance and mechanism of *in-situ* emulsification and viscosification system

To enhance the effectiveness of Janus nanoparticles, the surfactant IO and Tween 60 are chosen as the emulsifier. The construction of the *in-situ* emulsification and viscosification system was based on the principle of dispersive stability of the system. The assessment of dispersion stability was conducted using three distinct methodologies, including visual observation, particle size measurement, and the turbiscan stability index (TSI).

To determine the stability of nanofluids, the TSI values were determined using software in Turbiscan Lab Expert Stability Analyzer (Formulaction, France) (Li et al., 2019, 2020b). The TSI value can be achieved by:

$$\mathrm{TSI} = \sum_i \frac{\sum_h |T_i(h) - T_{i-1}(h)|}{H} \tag{1}$$

where i represents the number of scannings, h is the height of scanning, $T_i(h)$ is the transmission at height of h and i is the number of scanning, and H stands for the total height of the liquid in the sample cell. Thereby, lower TSI value suggests a more stable nano fluid.

The stability of the dispersion was observed by recording the volume of the oil phase separated out within 12 h in the oven. The viscosity was determined using a Brookfield viscometer (model DV2TLV, manufactured in the United States) at 25 °C and shear rate of 7 rad/s. The evolution of oil phase volume over time was recorded to assess the emulsifying capacity and emulsion stability . The microscopy was used to assess the agglomeration degree and droplet size of the emulsion droplets. The rheological characteristics of the emulsions were assessed using the HAAKE rheometer (MARS III, Germany) at 25 °C. The variations in the viscous modulus and elastic modulus as functions of the shear rate were determined.

2.4 Profile control effect of *in-situ* emulsification and viscosification system

To ascertain the efficacy of the enhanced oil recovery (EOR) effect and profile control effect, a series of experiments involving single-core and double-core flooding were conducted. The experimental protocol and procedures were outlined as follows:

The experimental setup involved the injection of an *in-situ* emulsification viscosification system with the concentration of 0.16 wt%. This concentration included 0.04 wt% Janus SiO_2 nanoparticles, 0.056 wt% Tween 60, and 0.064 wt% IO. The experiment was conducted using 50 mD core. An *in-situ* emulsification and viscosification system was injected in real time, with a total concentration of 0.16 wt%. The system consisted of 0.04 wt% Janus SiO_2 nanoparticles, 0.056 wt% Tween 60, and 0.064 wt% IO, respectively. The experiments were carried out using cores with permeabilities of 189 and 72 mD.

The dry weight of the core, measuring $4.5 \times 4.5 \times 30$ cm^3, was first recorded. The square core was subsequently evacuated and saturated with simulated formation water. The pore volume and porosity were afterwards calculated. The core was subjected to the injection of simulated formation water at a flow rate of 0.5 ml/min. The core's permeability was assessed by measuring the injection pressure and speed once the inject-

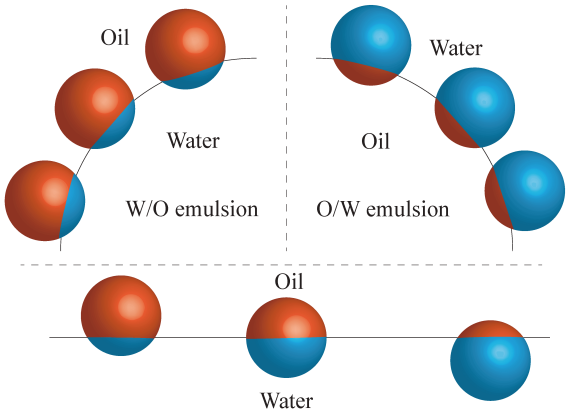

Fig. 2. Relationship between hydrophilic and hydrophobic degree of Janus nanoparticles and emulsion type.

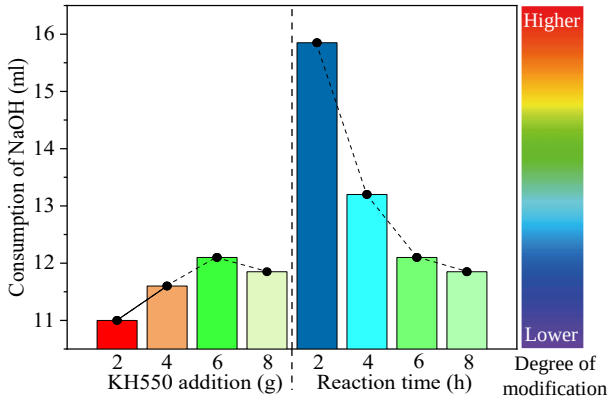

Fig. 3. Titration data of hydroxyl content on the surface of Janus SiO_2 nanoparticles.

ion pressure stabilized. For optimal distribution of oil and water in the core, crude oil should be introduced at a rate of 0.5 ml/min. This process should continue until bound water state. At this point, the pump should be stopped, and the cumulative water output should be recorded. After ageing for a period of one week, the core can be utilized for the following experiment. The injection rate for water flooding was established at 0.5 ml/min, the distribution and corresponding differential pressure were simultaneously recorded during this time interval. The pump was halted once the core water content reached 95%. The *in-situ* emulsification and viscosification system was initially injected with 0.5 pore volumes (PV) from the outlet with 0.5 ml/min. In the post water flooding experiment, the liquid production, oil production and corresponding differential pressure were recorded. The displacement experiment was halted once the water cut came to 98%, at the moment when the ultimate recovery was assessed.. The experiment was carried out at 90 °C and salinity of 35,000 ppm.

3. Results and discussions

3.1 Regulating principle of amphiphilicity for Janus SiO_2 nanoparticles

The amphiphilicity of Janus SiO_2 nanoparticles was adjusted to optimize the stability of the emulsion, and realize *in-situ* emulsification and viscosification. When nanoparticles exhibit stable adsorption on the interface, they tend to retain a significant portion of their surface within the external phase of the emulsion. This phenomenon arises from the varying surface wettability of the nanoparticles, enabling the formation of diverse emulsion types (Miyasaka et al., 2023). The larger the area occupied by nanoparticles is, the greater the energy requires for their desorption, which will affect the emulsion stability (Paternina et al., 2023). Emulsion type correlates with the hydrophilic and hydrophobic degree of Janus nanoparticles, see Fig. 2. Therefore, a series of nanoparticles exhibiting various degrees of hydrophilicity and hydrophobicity were synthesized, followed by an optimization for the modification degree based on emulsion stability.

The amino modification degree is characterized mainly by acid-base titration (see Fig. 3). The quantity of hydroxyl groups on the SiO_2 nanoparticle surface diminished as the extent of surface modification increased with longer reaction times across the four samples analyzed. With an increase in the KH550 addition amount, the quantity of hydroxyl groups on the SiO_2 surface rises, resulting in a diminished degree of modification. This is mainly attributed to the effect of the change in synthesis conditions on the hydrolysis-condensation equilibrium of the silane coupling agent KH550. In the lauric acid modification experiment, it is recommended to employ amino modified nanoparticles with 8 g KH550 and a reaction duration of 2 h.

The experimental results of SiO_2 modification degree by laurate amidation are located in Figs. 4(a)-4(b). The successful synthesis of Janus SiO_2 nanoparticles with varying degrees of modification was achieved through the manipulation of reaction time, addition of lauric acid, pH value adjustment, and catalyst addition. The observed water contact angle on Janus SiO_2 nanoparticles thin slices with surface water ranged from 96.2° to 130.8°. This is mainly attributed to the adjustment of the grafting density of lauric acid chain segments achieved by the change of synthesis conditions. When the contact angle of surface water exceeds 90°, Janus SiO_2 nanoparticles tends to stabilize the W/O emulsion. However, the strength of W/O emulsion stability and modification degree is not directly proportional to the contact angle. Later, the degree of modification will be optimized.

Nanofluids were synthesized through the dispersion of Janus SiO_2 nanoparticles in deionized water under ambient conditions. The nanofluid was mixed with crude oil in order to create a W/O emulsion. The emulsion morphology at 0 and 24 h was observed under room temperature conditions, as depicted in Fig. 5(a)-5(b). In Fig. 5(a)-5(b), the light brown region represents for the emulsion itself, while the dark brown region indicates the quantity of oil phase that has been released from the emulsion through the process of demulsification. At 0 h, Janus SiO_2 nanoparticles with varying degrees of modification are all capable of effectively producing W/O emulsions. Furthermore, the resulting emulsion exhibits a uniform appearance. A significant difference in

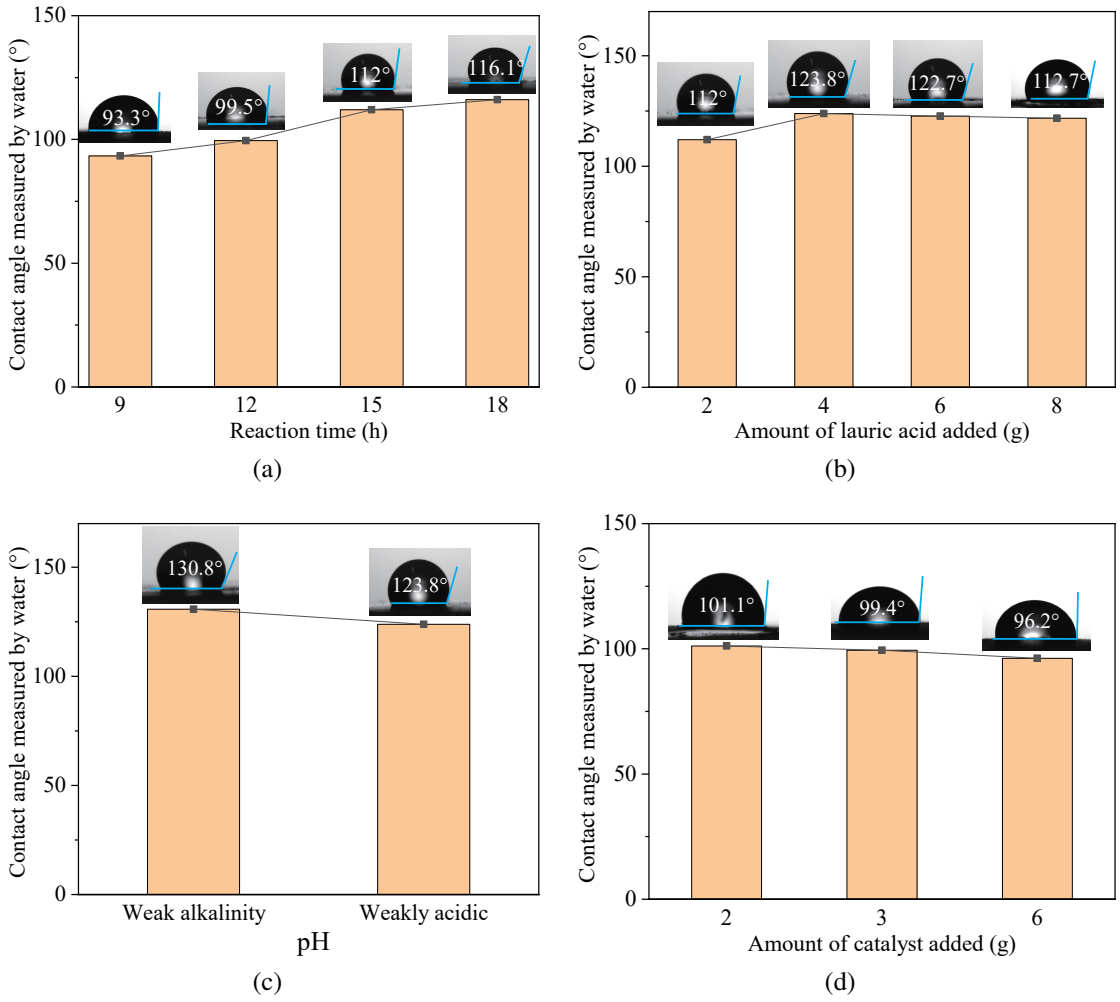

Fig. 4. Surface water contact angles on amphiphilic Janus SiO_2 nanoparticles thin slices prepared under various reaction conditions. (a) Reaction time, (b) lauric acid addition, (c) pH value and (d) amount of catalyst added.

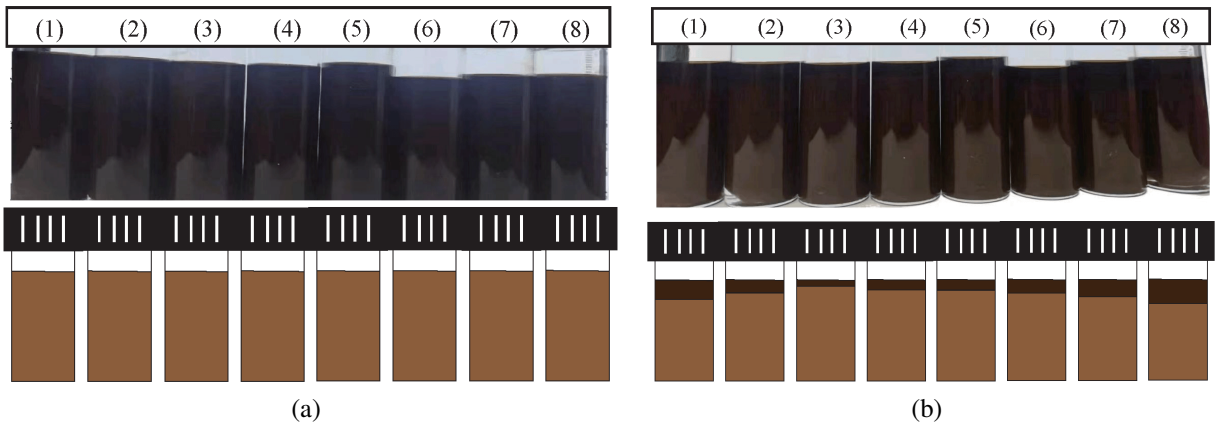

Fig. 5. Amphiphilic Janus SiO_2 nanoparticles stabilized W/O emulsions at (a) 0 h and (b) 24 h. (Water contact angles of Janus SiO_2 nanoparticle surface (1) 99.5°, (2) 112 °, (3) 116.1 °, (4) 112.7°, (5) 123.8°, (6) 101.1 °, (7) 99.4° and (8) 96.2°).

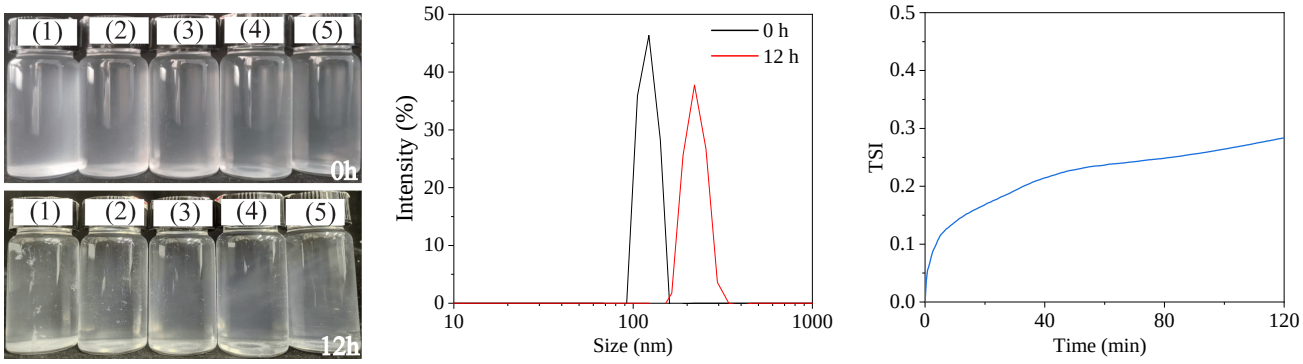

(a) (b) (c)

Fig. 6. (a) Dispersion stability of the system composed of 0.05% Janus SiO_2 nanoparticles and 0.15% Tween 60/ IO surfactant at various Tween 60/ IO molar ratios in aqueous phase at 90 °C and 35,000 ppm salinity ((1) 1:9, (2) 2:8, (3) 3:7, (4) 4:6 and (5) 5:5), (b) particle size test results at 0 and 12 h of *in-situ* emulsion and viscosification system and (c) change in TSI value of *in-situ* emulsification and viscosification system within 2 hrs.

emulsion stability, influenced by nanoparticles with differing modification levels, was observed after 24 h. One notable observation is that the emulsion exhibited superior stability when the Janus SiO_2 nanoparticles performed a surface water contact angle of 116.1°, resulting in the lowest amount of oil leaching. The experimental findings indicate that a weakly oil-wet surface wettability of the nanoparticles leads to the stabilization of a water-in-oil emulsion by the nanoparticles. To optimize interface activity and emulsion stability of Janus SiO_2 nanoparticles, a surface modification degree of 116.1° is selected for system construction.

3.2 *In-situ* emulsion and viscosification system build and performance testing

The dispersion stability of the *in-situ* emulsion and viscosification system is improved under high-temperature and high-salt. Fig. 6(a) displays the results of the assessment of dispersion stability for the *in-situ* emulsification and viscosification system through the visual method. The *in-situ* emulsification and viscosification systems exhibited favorable dispersion stability when the molar ratio of Tween 60 to IO exceeded 3:7. Figs. 6(b)-6(c) displays the measured results of particle size and TSI data for the *in-situ* emulsification and viscosification system. The particle size of the *in-situ* emulsification and viscosification system changed little within 12 hours, and the overall dispersion stability nearly unchanged as is reflected by the TSI value.

A robust adsorption layer of Tween 60 and IO formed on the surface of Janus SiO_2 nanoparticles is largely responsible for the system's remarkable dispersion stability. The adsorption layer enhances the quantity of surfactant adsorbed, resulting in a stable system structure after adsorption (Kumar et al., 2020; Venancio et al., 2020). As a consequence of the solubility issue, a portion of IO undergoes dissolution in water and subsequent hydrolysis, while another portion remains suspended in water in the form of min droplets, as depicted in Figs. 7(a)-7(b). There are three types of surfactants exist in aqueous solutions, including IO molecule in its unhydrolyzed state and the hydroxyethyl IO compound that is formed after hydrolysis, as well as the anionic surfactant oleate. These three surfactants and the week electro-positive Tween 60 are co-adsorbed on the surface of Janus SiO_2 nanoparticles through hydrophobic interactions, electrostatic interactions , and hydrogen bonding. This results in the formation of a compact adsorption layer consisting of Tween 60 with hydrophilic groups, which in turn creates a solvation layer on the surface of the nanoparticles (Nazari et al., 2019; Xie et al., 2020; Xu et al., 2023). The overlapping of solvation layers between particles gives rise to repulsive forces, resulting in the improved stability and dispersion of nanoparticles, as depicted in Fig. 7(c). The process of adsorption, wherein surfactant molecules adhere to particles, serves to enhance the stable dispersion of the surfactant in an aqueous solution, thereby preventing precipitation.

Figs. 8(a)-8(b) depict the stability of emulsions that were prepared using various concentrations of *in-situ* emulsification and viscosification systems. For all concentrations, *in-situ* emulsification and viscosification systems have the capability to generate W/O emulsions. Furthermore, these emulsion systems can sustain their stability for a duration of 12 hrs without any noticeable demulsification. In Fig. 8(c) of the emulsion viscosification effect test, it is observed that the *in-situ* emulsion and viscosification concentration system at 0.64 wt% exhibits the most favourable viscosification effect. Specifically, the W/O emulsion stabilized by 0.64 wt% system displayed the viscosity of 4,960 mPa·s.

In order to further validate the variation in emulsification effects among various concentration systems, microscopy was utilized to examine the microscopic structure of the emulsion. The experimental findings are depicted in Figs. 9(a)-9(e). When the concentration of the *in-situ* emulsification and viscosification system is 0.64 wt%, the resulting emulsion droplet exhibits the smallest particle size and a high packing density, indicating enhanced emulsion viscosity and stability.

Figs. 10(a)-10(b) display the elastic and viscous modulus of emulsions that have been prepared using various concen-

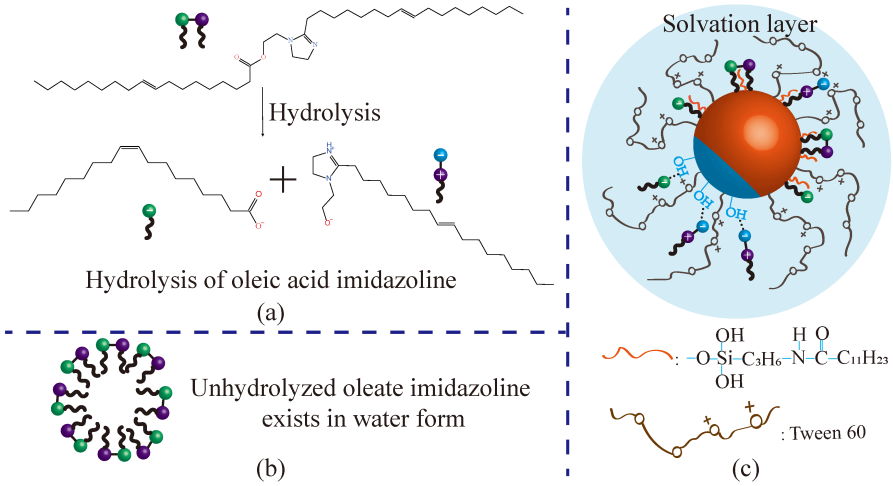

Fig. 7. (a) Sketch of IO hydrolysis in the water, (b) the present form of unhydrolyzed IO in water and (c) schematic diagram of the dispersing mechanism for the *in-situ* emulsion and viscosification system.

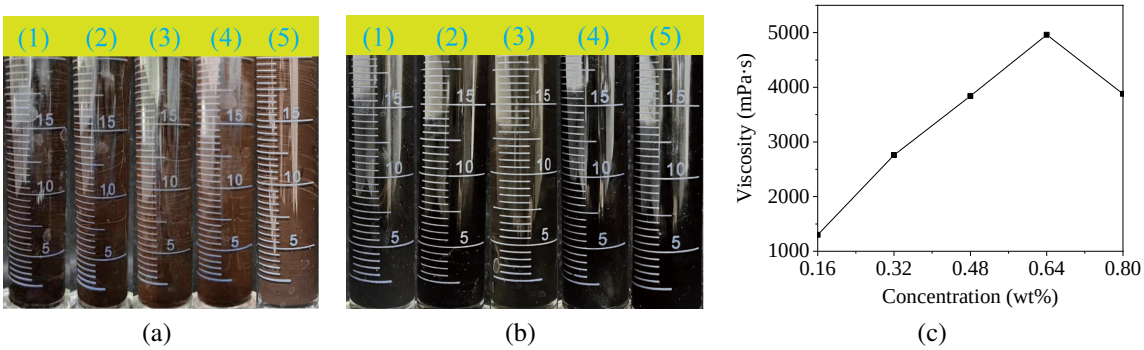

Fig. 8. (a) and (b) Emulsion morphology of *in-situ* emulsification and viscosification system with various concentrations, (c) the viscosification effect of the prepared emulsions with different concentration systems.

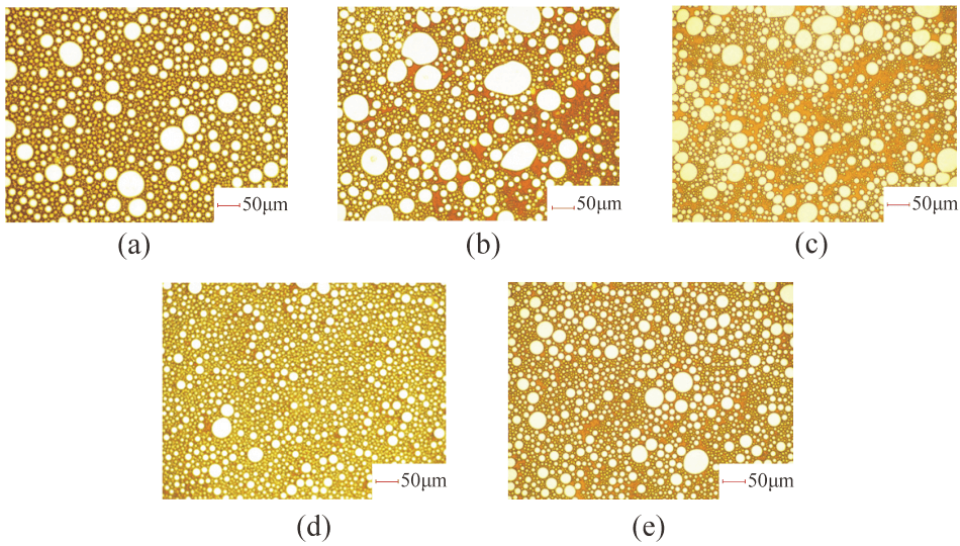

Fig. 9. For the preparation of emulsion concentration system microstructure: (a) 0.16 wt%, (b) 0.32 wt%, (c) 0.48 wt%, (d) 0.64 wt% and (e) 0.80 wt%.

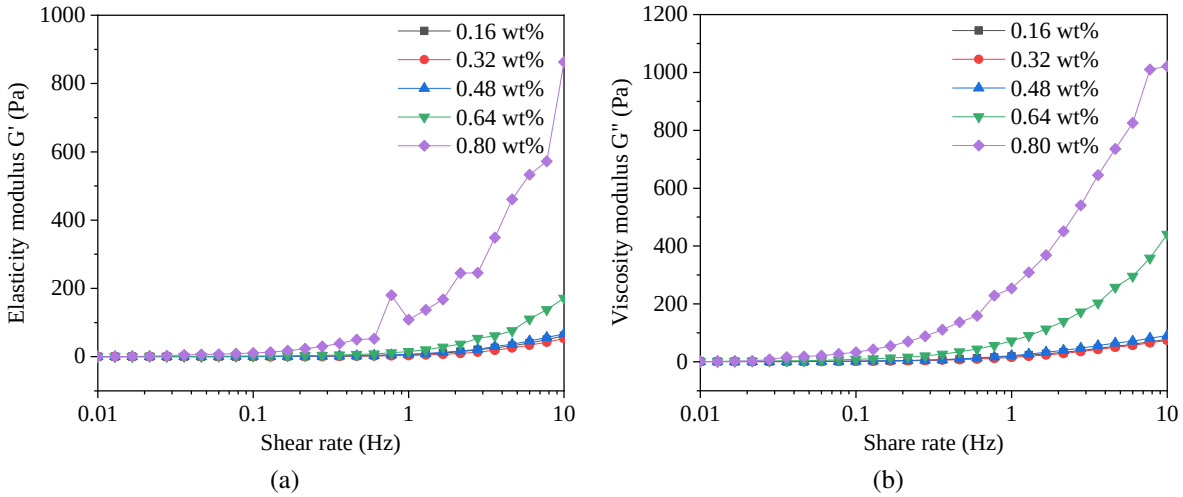

Fig. 10. (a) and (b) The elastic and viscous modulus of W/O emulsions prepared by *in-situ* emulsification and viscosification system with various concentrations.

trations. The data presented in Figs. 10(a)-10(b) demonstrate a positive correlation between the system concentration and both the viscous modulus and elastic modulus. The higher viscous modulus facilitates improved flowability, allowing the emulsion to flow until the channel becomes obstructed by emulsion droplets. When the emulsion droplets obstruct the pore roar and impede the flow, they demonstrate elastic behavior, thereby augmenting the strength of plugging. As the shear rate increases, both the viscous modulus and elastic modulus exhibit an increase trend.

To clarify the mechanism of *in-situ* emulsification and viscosification system, the dynamic adsorption process and phase transformation process of surfactant were analyzed from the perspective of emulsification. The unique bridge structure of Janus nanoparticle stabilized emulsion was analyzed from the perspective of emulsion stability.

Firstly, Janus SiO_2 nanoparticles with surfactants adsorbed on the surface and small IO droplets will spontaneously adsorb at the interface during the water-oil collision (Fainerman et al., 2020). Since the solubility of IO surfactant in oil is greater than that in water, the dynamic adsorption-desorption behavior of surfactant occurs between the oil-water interface and the oil phase (Yang et al., 2020; Paternina et al., 2023), and the concentration of surfactant in the oil phase increases significantly, as shown in Figs. 11(a)-11(b), which is important for the generation of *in-situ* W/O emulsion in the formation. The observed outcomes result from the synergistic interaction between surfactants and Janus SiO_2 nanoparticles. The increased interfacial activity and enhanced adsorption of Janus SiO_2 nanoparticles at the interface result from their amphiphilic structure and the adsorption of surfactants onto their surface. (Sircar et al., 2022; Vu et al., 2022).In the formation, the crude oil emulsifies to prepare a W/O/W emulsion with an outer layer stabilized by Tween 60 and an inner layer stabilized by Janus SiO_2 nanoparticles and IO (Wei et al., 2020; Nafisifar et al., 2023). When droplets collide with each other, the oil phase between different droplets will coalesce with each other due to the poor stability of the emulsion stabilized by Tween 60 (Farooq et al., 2019). The inner droplets stabilized by Janus SiO_2 nanoparticles and IO, due to the irreversible adsorption of particles (Lu et al., 2020) and the formation of dense adsorption layer (Cui et al., 2023) between surfactant and nanoparticles at the interface, the interfacial layer is stable, and the inner phase water droplets will not agglomerate. The irreversible adsorption of Janus nanoparticles is mainly since its maximum adsorption energy at the interface is three times that of isotropic particles at the interface, which enables it to be strongly fixed at the interface (Gao et al., 2014; Borówko et al., 2023). As shown in Fig. 11c, the emulsion viscosity will be significantly greater than the crude oil due to the mutual extrusion and friction between the droplets after the droplet oil converges and merges (Lu et al., 2023b).

Furthermore, the simultaneous co-adsorption of nanoparticles and surfactants at the interface leads to a large packing density of the interfacial film. The substantial interfacial adsorption energy exhibited by nanoparticles prevents desorption from the interface. Consequently, nanoparticles assume a prominent role in maintaining the emulsions stability (Hu et al., 2018; Tran et al., 2022). Additionally, as the oil phase undergoes gradual separation, the proximity of the droplets leads to the formation of a distinctive structure wherein Janus SiO_2 nanoparticles contribute to the reduction of IFT and enhance surface wettability. This structure facilitates the bridging of oil droplets between nanoparticles, which significantly contributes to the high stability of the W/O emulsion during subsequent processes. The difference in wettability between the two hemispheres of Janus SiO_2 nanoparticles leads to distinct bending curvatures of the interface. The oil contact angle of the hydrophilic hemisphere is larger than that of the hydrophobic side ($\alpha > \beta$, see Fig. 11(e)). This phenomenon is observed when the Janus SiO_2 nanoparticles simultaneously stabilize two emulsion droplets, as depicted in Figs. 11(d)-11(e).

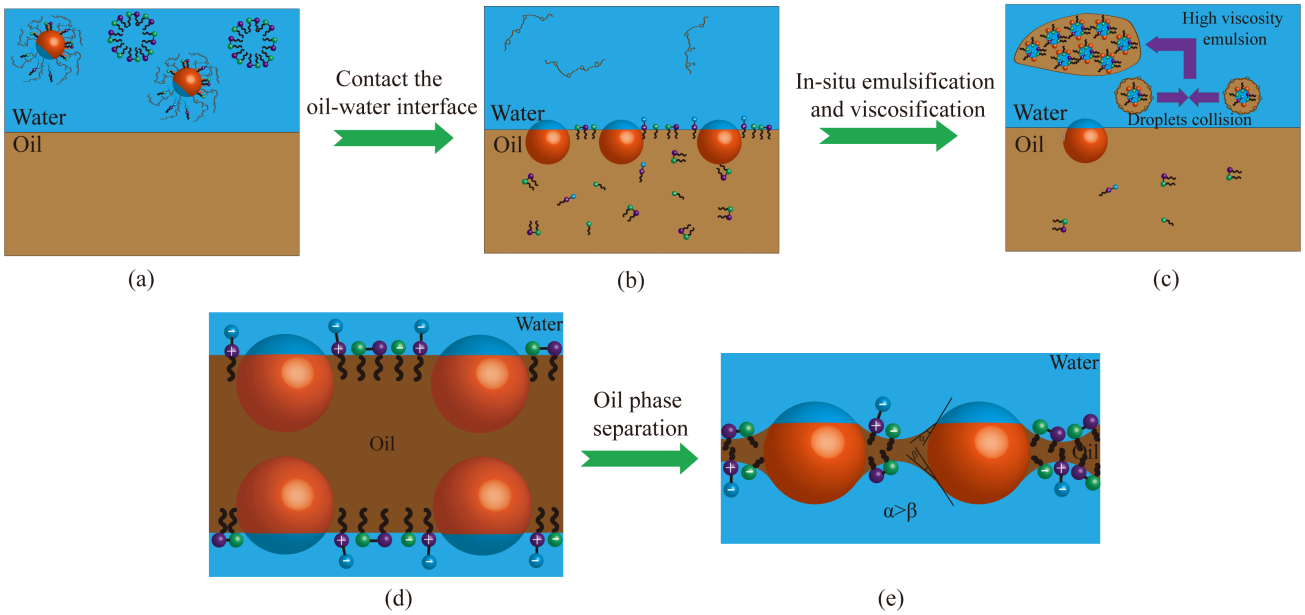

Fig. 11. Emulsification and stabilizing mechanism enabled by the *in-situ* emulsification and viscosification system. (a) The stable state of *in-situ* emulsification and viscosification system in water, (b) adsorption and mass transfer of surfactants and Janus nanoparticles at interface, (c) emulsification and droplet coalescence, (d) the interface formed dense adsorption layer and (e) the oil droplets are bridged by nanoparticles.

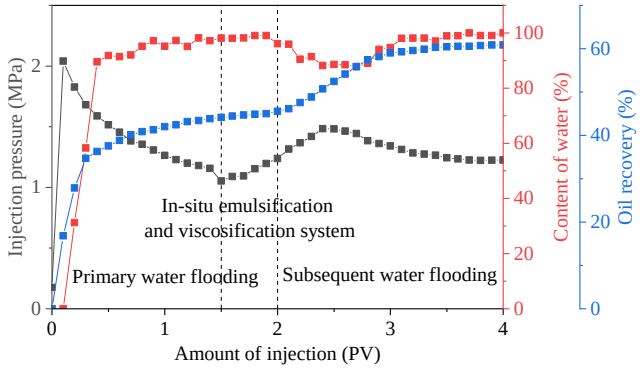

Fig. 12. Experiment results of 38 mD single core physical model.

3.3 Profile control effect of *in-situ* emulsion and viscosification system

As depicted in Fig. 12, the single core physical model experiment was conducted using core with a permeability of 38 mD. Following the introduction of an *in-situ* emulsification and viscosification system, the displacement pressure and oil recovery rate exhibited significant improvements. Specifically, the recovery rate experienced a notable increase of 16.71%, while the injection pressure rose from 1.05 to 1.48 MPa. The *in-situ* emulsification and viscosification system exhibited a notable plugging effect and oil displacement effect. The utilization of the *in-situ* emulsification and viscosification system improved oil recovery.

The experimental results of the double-core physical model experiment are shown in Fig. 6(b). The experiment was conducted using square cores measuring 189 and 72 mD. Following the injection of 0.5 PV of an *in-situ* emulsification and viscosification system, the injection pressure experienced a substantial increase, rising from 0.05 to 0.35 MPa. This increase in pressure effectively initiated the low permeability layer. Following the regulation of *in-situ* emulsion and viscosification system, the high permeability layer experienced a notable increase of 12.98%, while the oil recovery efficiency of the low permeability layer also exhibited a significant improvement of 12.86%.

Janus SiO_2 nanofluid flooding is acknowledged as an effective method for enhancing oil recovery in low-permeability reservoirs. (Li et al., 2023). The enhanced oil recovery mechanisms include structural separation pressure, IFT reduction, emulsification, and emulsion stability (Jia et al., 2021). This work reveals a new mechanism of Janus SiO_2 nanofluids in EOR process from a new perspective. By complexing Janus SiO_2 nanoparticles with surfactants, *in-situ* emulsification was achieved via generation of high-viscosity W/O emulsion. Through droplet plugging, droplet bridging and high-viscosity W/O emulsion slug, achieved profile control and the macroscopic sweeping volume was increased. The plugging mechanism of the *in-situ* emulsification and viscosification system within the hyperosmotic channel is shown in Fig. 14.

4. Conclusions

In current work, an *in-situ* emulsification and viscosification system utilizing Janus SiO_2 nanoparticles and surfactants was proposed. The profile control effect through *in-situ* emulsification and viscosification can be attributed to synergistic effect between Janus SiO_2 nanoparticles/surfactant system. The primary findings can be summarized as follows:

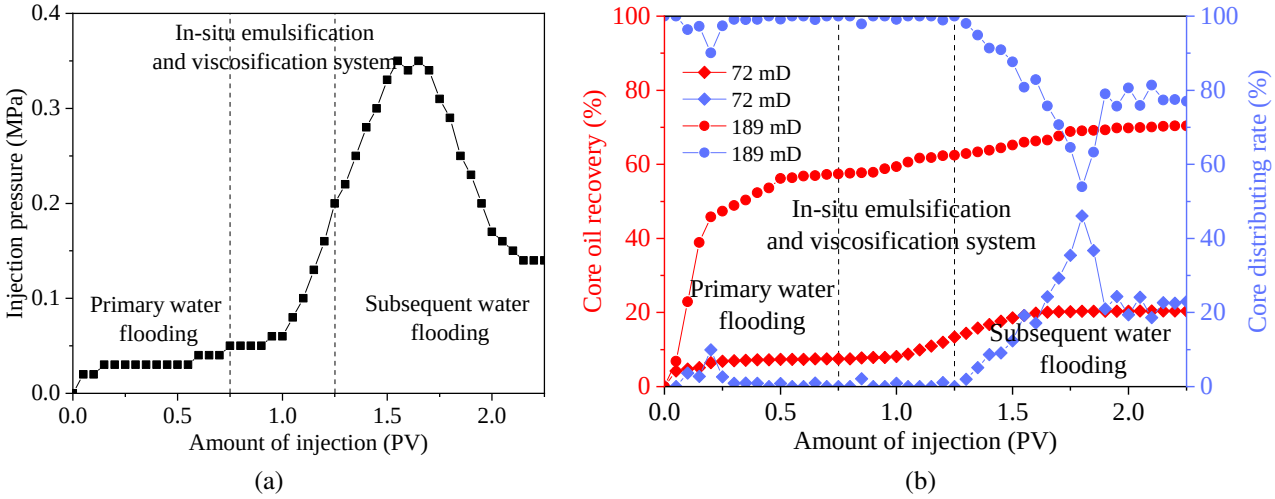

Fig. 13. Double-core parallel physical model experiments with 72 and 189 mD cores. (a) The change of injection pressure with injection volume and (b) variation of oil recovery and diversion rate of different cores.

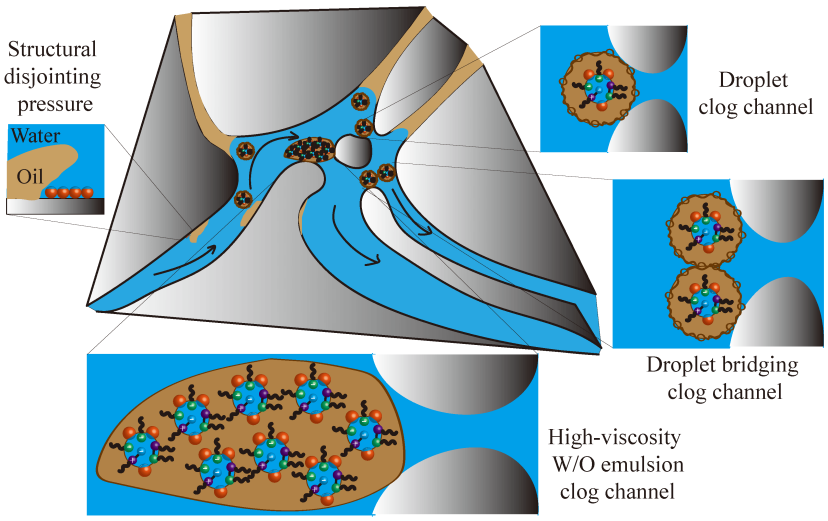

Fig. 14. Profile control and EOR mechanism of *in-situ* emulsification and viscosification system.

1) By manipulating the modification degree, amphiphilic Janus SiO_2 nanoparticles with varying hydrophilic and hydrophobic properties were synthesized. The W/O emulsion stability was the highest when the contact angle of amphiphilic Janus SiO_2 nanoparticles with the surface water reached 116.1°.
2) The *in-situ* emulsification and viscosification system consisting of IO, Tween 60, and amphiphilic Janus SiO_2 nanoparticles were proposed. The mechanism of *in-situ* emulsification and viscosification system was elucidated from two aspects: The dynamic adsorption and phase conversion of surfactant, and the unique bridge structure of Janus nanoparticle stabilized emulsion.
3) The profile control performance of the system were evaluated by core flooding experiments with both single-core and double-core configurations. The *in-situ* emulsification and viscosification system showed an enhanced profile control efficacy in low permeability.

Acknowledgements

This work was financially supported by National Natural Science Foundation of China (No. 52374053) and Beijing Municipal Excellent Talent Training Funds Youth Advanced Individual Project (No. 2018000020124G163).

Conflict of interest

The authors declare no competing interest.

References

Borówko, M., Staszewski, T., Tomasik, J. Janus Ligand-Tethered Nanoparticles at Liquid-Liquid Interfaces. Journal of Physical Chemistry B, 2023, 127(22): 5150-5161.

Cao, J., Chen, Y., Wang, X., et al. Janus sulfonated graphene oxide nanosheets with excellent interfacial properties for enhanced oil recovery. Chemical Engineering Journal, 2022, 443: 136391.

Chen, H., Ji, B., Wei, B., et al. Experimental simulation of enhanced oil recovery on shale rocks using gas injection from material to Characterization: challenges and solutions. Fuel, 2024, 356: 129588.

Chen, L., Zhang, G., Ge, J., et al. Property evaluation of a new selective water shutoff agent for horizontal well. Colloids and Surfaces A: Physicochemical and Engineering Aspects, 2014, 446: 33-45.

Choi, J., Kim, H., Lee, H., et al. Hydrophobically modified silica nanolaces-armored water-in-oil pickering emulsions with enhanced interfacial attachment energy. Journal of Colloid and Interface Science, 2023, 641: 376-385.

Cui, S., Yang, Z., McClements, D. J., et al. Stability mechanism of Pickering emulsions co-stabilized by protein nanoparticles and small molecular emulsifiers by two-step emulsification with different adding sequences: From microscopic to macroscopic scales. Food Hydrocolloids, 2023, 137: 108372.

Fainerman, V. B., Aksenenko, E. V., Kovalchuk, V. I., et al. New view of the adsorption of surfactants at water/alkane interfaces - Competitive and cooperative effects of surfactant and alkane molecules. Advances in Colloid and Interface Science, 2020, 279: 102143.

Farooq, A., Shafaghat, H., Jae, J., et al. Enhanced stability of bio-oil and diesel fuel emulsion using Span 80 and Tween 60 emulsifiers. Journal of Environmental Management, 2019, 231: 694-700.

Gao, H., Lu, Z., Liu, H., et al. Orientation and surface activity of Janus particles at fluid-fluid interfaces. Journal of Chemical Physics, 2014, 141(13): 134907.

Guo, P., Tian, Z., Zhou, R., et al. Chemical water shutoff agents and their plugging mechanism for gas reservoirs: A review and prospects. Journal of Natural Gas Science and Engineering, 2022, 104: 104658.

Hu, P., Jia, Z., Shen, Z., et al. High dielectric constant and energy density induced by the tunable TiO_2 interfacial buffer layer in PVDF nanocomposite contained with core-shell structured TiO_2@$BaTiO_3$ nanoparticles. Applied Surface Science, 2018, 441: 824-831.

Jia, H., Dai, J., Miao, L., et al. Potential application of novel amphiphilic Janus-SiO_2 nanoparticles stabilized O/W/O emulsion for enhanced oil recovery. Colloids and Surfaces A: Physicochemical and Engineering Aspects, 2021, 622: 126658.

Krishnakumar, V., Elansezhian, R. Dispersion stability of zinc oxide nanoparticles in an electroless bath with various surfactants. Materials Today: Proceedings, 2022, 51: 369-373.

Kumar, A., Park, B. J., Tu, F., et al. Amphiphilic Janus particles at fluid interfaces. Soft Matter, 2013, 9(29): 6604-6617.

Kumar, R. S., Chaturvedi, K. R., Iglauer, S., et al. Impact of anionic surfactant on stability, viscoelastic moduli, and oil recovery of silica nanofluid in saline environment. Journal of Petroleum Science and Engineering, 2020, 195: 107634.

Li, J., Wang, Z., Yang, H., et al. Compatibility evaluation of in-depth profile control agents in dominant channels of low-permeability reservoirs. Journal of Petroleum Science and Engineering, 2020a, 194: 107529.

Li, S., Braun, O., Lauber, L., et al. Enhancing oil recovery from high-temperature and high-salinity reservoirs with smart thermoviscosifying polymers: A laboratory study. Fuel, 2021a, 288: 119777.

Li, X., Gao, D., Liu, M., et al. Synthesis of amphiphilic Janus SiO_2/styrene butyl acrylate polymer microspheres and their application in oil recovery. Colloids and Surfaces A: Physicochemical and Engineering Aspects, 2023, 675: 132076.

Li, Y., Du, N., Song, S., et al. Size-dependent dissociation of surface hydroxyl groups of silica in aqueous solution. Colloids and Surfaces A: Physicochemical and Engineering Aspects, 2021b, 629: 127446.

Li, Z., Kang, W., Bai, B., et al. Fabrication and Mechanism Study of the Fast Spontaneous Emulsification of Crude Oil with Anionic/Cationic Surfactants as an Enhanced Oil Recovery (EOR) Method for Low-Permeability Reservoirs. Energy & Fuels, 2019, 33(9): 8279-8288.

Li, Z., Wu, H., Hu, Y., et al. Ultra-low interfacial tension biobased and catanionic surfactants for low permeability reservoirs. Journal of Molecular Liquids, 2020b, 309: 113099.

Lu, J., Pu, W., He, W., et al. Progress in research of sulfobetaine surfactants used in tertiary oil recovery. Journal of Surfactants and Detergents, 2023a, 26(4): 459-475.

Lu, S., Yang, D., Wang, M., et al. Pickering emulsions synergistic-stabilized by amphoteric lignin and SiO_2 nanoparticles: Stability and pH-responsive mechanism. Colloids and Surfaces A: Physicochemical and Engineering Aspects, 2020, 585: 124158.

Lu, Y., Zhang, R., Jia, Y., et al. Effects of nanoparticle types and internal phase content on the properties of W/O emulsions based on dual stabilization mechanism. Food Hydrocolloids, 2023b, 139: 108563.

Miyasaka, K., Imai, Y., Tajima, K. Preparation of oil-in-water and water-in-oil emulsions with the same composition using hydrophilic nanoparticles by three-phase emulsification. Colloids and Surfaces A: Physicochemical and Engineering Aspects, 2023, 670: 131598.

Nafisifar, A., Manshad, A. K., Shadizadeh, S. R. Synergistic study of xanthan-gum based nano-composite on PELS anionic surfactant performance, and mechanism in porous media: Microfluidic & carbonate system. Fuel, 2023, 348: 128510.

Nazari, B., Ranjbar, Z., Moghaddam, A. R., et al. Dispersing graphene in aqueous media: Investigating the effect of different surfactants. Colloids and Surfaces A: Physicochemical and Engineering Aspects, 2019, 582: 123870.

Pang, B., Liu, H., Liu, P. W., et al. Water-in-oil Pickering emulsions stabilized by stearoylated microcrystalline cellulose. Journal of Colloid and Interface Science, 2018, 513: 629-637.

Paternina, C. A., Quintero, H., Mercado, R. Improving the interfacial performance and the adsorption inhibition of an extended-surfactant mixture for enhanced oil recovery using different hydrophobicity nanoparticles. Fuel, 2023, 350: 128760.

Shen, H., Yang, Z., Wang, G., et al. 2D Janus polymer nanosheets for enhancing oil recovery: From material preparation to property evaluation. Petroleum Science, 2023, 20(3): 1584-1597.

Sircar, A., Rayavarapu, K., Bist, N., et al. Applications of nanoparticles in enhanced oil recovery. Petroleum Research, 2022, 7(1): 77-90.

Tran, T., Perdomo, M. E. G., Haghighi, M., et al. Study of the synergistic effects between different surfactant types and silica nanoparticles on the stability of liquid foams at elevated temperature. Fuel, 2022, 315: 122818.

Venancio, J. C. C., Nascimento, R. S. V., Perez-Gramatges, A. Colloidal stability and dynamic adsorption behavior of nanofluids containing alkyl-modified silica nanoparticles and anionic surfactant. Journal of Molecular Liquids, 2020, 308: 113079.

Vu, T. V., Razavi, S., Papavassiliou, D. V. Effect of Janus particles and non-ionic surfactants on the collapse of the oil-water interface under compression. Journal of Colloid and Interface Science, 2022, 609: 158-169.

Wei, Y., Tong, Z., Dai, L., et al. Novel colloidal particles and natural small molecular surfactants co-stabilized Pickering emulsions with hierarchical interfacial structure: Enhanced stability and controllable lipolysis. Journal of Colloid and Interface Science, 2020, 563: 291-307.

Wu, H., Gao, K., Lu, Y., et al. Silica-based amphiphilic Janus nanofluid with improved interfacial properties for enhanced oil recovery. Colloids and Surfaces A: Physicochemical and Engineering Aspects, 2020, 586: 124162.

Xie, S., Chen, S., Zhu, Q., et al. Janus nanoparticles with tunable amphiphilicity for stabilizing pickering-emulsion droplets via assembly behavior at oil-water interfaces. ACS Applied Materials & Interfaces, 2020, 12(23): 26374-26383.

Xu, G., Chang, J., Wu, H., et al. Enhanced oil recovery performance of surfactant-enhanced Janus SiO_2 nanofluid for high temperature and salinity reservoir. Colloids and Surfaces A: Physicochemical and Engineering Aspects, 2023, 657: 130545.

Yang, H., Lv, Z., Wang, L., et al. Stability mechanism of controlled acid-resistant hydrophobic polymer nanospheres on CO_2 foam. Fuel, 2023a, 346: 128332.

Yang, X., Chen, A., Mao, J., et al. Synthetic polymer fracturing fluid weighted by sodium formate enables fracture stimulations in Ultra-High pressure and High-Temperature reservoir. Fuel, 2023b, 353: 129170.

Yang, Y., Ma, Z., Xia, F., et al. Adsorption behavior of oil-displacing surfactant at oil/water interface: Molecular simulation and experimental. Journal of Water Process Engineering, 2020, 36: 101292.

Yarveicy, H. Effect of nanoparticles on phase behavior of surfactant-oil-water system: An application in multiphase flow system. Advances in Geo-Energy Research, 2023, 9(3): 152-155.